

Serviceability-Based Flexural Design of UHPC Beams

Chidchanok Pleesudjai¹, Devansh Deepak Patel¹, Barzin Mobasher³,

¹ Graduate Research Associate, School of Sustainable Engineering and Built Environment, Arizona State University, Tempe, AZ 85287-8706, USA, cpleesud@asu.edu, dpatel52@asu.edu

³ Professor, School of Sustainable Engineering and Built Environment, Arizona State University, Tempe, AZ 85287-8706, USA, barzin@asu.edu. ORCID <https://orcid.org/0000-0002-7580-2855>

Abstract

A paradigm shift is required in the design of sustainable structures utilizing UHPC. Using a combination of new materials formulations and closed-form analysis procedures to calculate the load-deflection response of a structure, limit-state designs aimed at the long-term durability of UHPC cement composite systems are proposed. The perspective is to meet the traditional ultimate design criteria and emphasize the perspective on serviceability measures defined in terms of durability, deflection, stiffness, and performance aspects under the service loads. Three main stages of sustainable product development will be addressed using the material properties of non-proprietary UHPC. The influence of fiber type, matrix modifications, and processing parameters under tensile and flexural loading are incorporated in constitutive material properties. The enhanced tensile behavior in the post-cracking stage is primarily governed by mechanical anchorage and bond characteristics between matrix and fibers. The residual strength under flexural loads, allows for the distribution of localization and results in additional cracking. The significant delays in stiffness loss and damage localization allows for deflection hardening applications. Innovative methods of design using combinations of reinforcement and UHPC materials are presented.

Keywords: structural design, strain hardening, strain softening, flexural response, moment-curvature, load-deflection, serviceability

1. Introduction

Ultra high-performance concrete (UHPC) is a developing category of cement-based composites with fibers that exhibit exceptional mechanical strength and durability when compared to conventional concrete and other fiber-reinforced alternatives (Haber, Varga, Graybeal, Nakashoji, & El-Helou, 2018). The compressive and flexural strength can be significantly improved compared to the normal concrete class by reducing the w/c, minimizing porosity, improving packing density, and using fiber reinforcement. UHPC use is recommended for high-strength and durability applications in critical structures such as bridges, tunnel segments, blast-resistant, or structures that face harsh environments (Wille & Naaman, 2012). The enhanced strength properties can potentially reduce costs by diminishing material volume, load demands, section sizes, labor, and

construction time, and may even eliminate the need for the number of girders or intermediate piers in bridge applications (El-Helou & Graybeal, 2021). The low porosity of UHPC provides resistance to water penetration and chemical attack, hence higher durability. The high volume of short steel fibers in a UHPC mixture improves the mechanical response by increasing the stiffness and residual strength in the serviceability range (Le Hoang & Fehling, 2017).

Figure 1 shows typical load-deflection curves with the cracking mechanism in UHPC at different stages (Mobasher, Li, Yao, Arora, & Neithalath, 2021). Note that the plain UHPC is extremely brittle, however addition of fibers can result in an elastirc prefrectly plastic material with several stages of crack initiation and growth, debonding and pullout as well as multiple crack distribution.

Design of UHPC materials should consider serviceability limits-states that incorporate initial post-cracking stiffness and deflection control from the fibers since the long-term durability of components under service load is an important feature of infrastructure. The presented model incorporates an objective definition of serviceability limit states based on user-defined and specified strain, crack width, deflection, or curvature ductility. Design for serviceability requires a better understanding of the load path and state of nonlinear behavior vis-à-vis cracking. Determination of design parameters such as load capacity at a certain level in the load-deformation history is, therefore, an important aspect of the modeling.

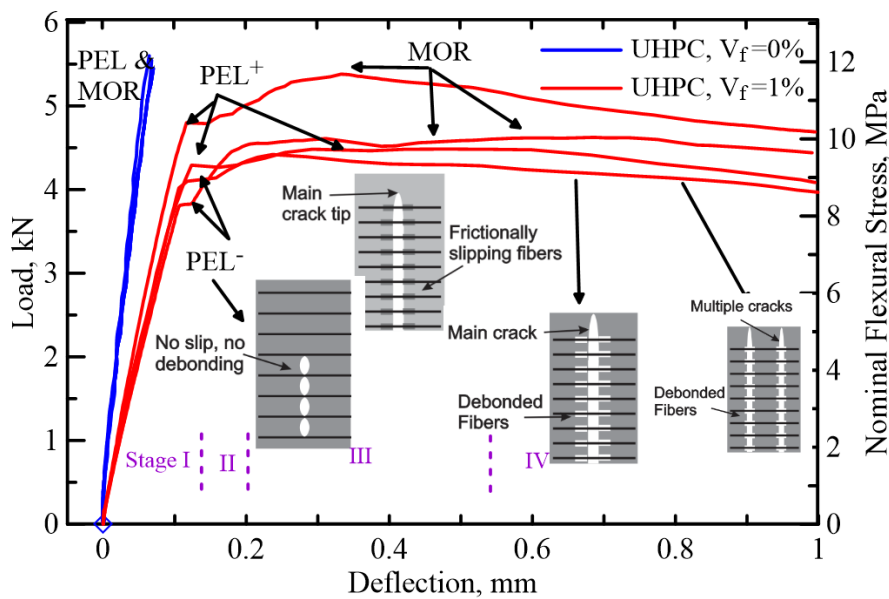


Figure 1. Stages of cracking of UHPC beam with fibers vs. without fibers

2. Material Model

The constitutive model of UHPC is simplified into the context of multi-linear segments in order to yield the closed-form of moment-curvature response at Serviceability Limit State (SLS). Tensile stress-strain curve is described by three segments of linear equations called “Tri-linear model”, by the coordinates in tension (σ_{cr} , σ_1 , σ_{tu}) where the σ_1 and σ_{tu} are adjustable to represent strain softening or hardening response of the residual tensile strength of UHPC. Two linear segments are used to represent elastic perfectly plastic response of compressive stress-strain model and it is controlled by two coordinates (σ_{cy} , σ_{cu}). The tensile and compressive model of continuous

reinforcement bars is defined by two linear segments with elastic response and yield behavior at f_{sy} . The model can be adjusted by varying the material parameters to imitate CFRP or GFRP bars.

Figure 2 presents the material model with two intrinsic parameters, tensile modulus E and first cracking tensile strain ε_{cr} with all other parameters normalized with respect to them. The tension model elastic range extends up to the first cracking coordinates $(\varepsilon_{cr}, \sigma_{cr})$ as seen in Figure 2(a). The non-dimensional variable of tensile strains is defined as β , as $\varepsilon_t = \beta \varepsilon_{cr}$ with elastic response defined as $\beta \leq 1$ and post-crack region as $\beta > 1$. The stiffness of post-cracking modulus uses η_l where $E_{cr} = \eta_l E$ is defined by the positive and negative values of η_l for strain-hardening or softening. The transition from the second to the third region occurs at the strain parameter, $\beta_l = \varepsilon_{tm}/\varepsilon_{cr}$, and followed by a constant residual strength as $\sigma_{tu} = \mu \sigma_{cr} = \mu \varepsilon_{cr} E$. The tensile response terminates at the ultimate strain $\varepsilon_{tu} = \beta_{tu} \varepsilon_{cr}$.

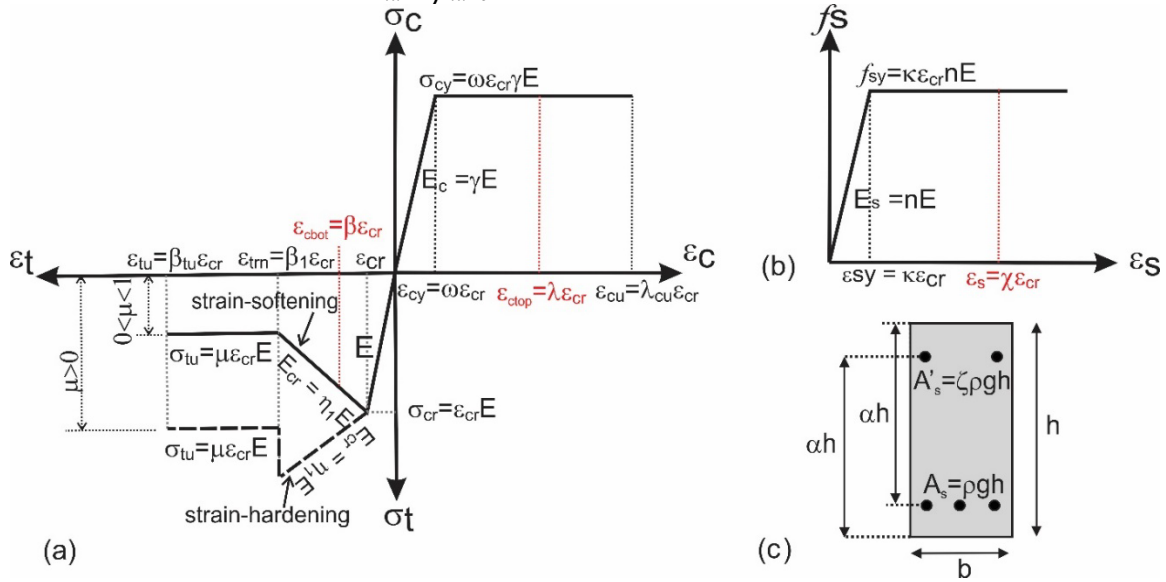


Figure 2. Material model for doubly reinforced concrete design (a) Tension model and Compression model; (b) Continuous reinforcement model; (c) Beam cross-section.

The elastic-perfectly plastic compression response is illustrated in Figure 2(a) with a modulus $E_c = \gamma E$. The stress and strain associated with the ultimate strength are defined as $\omega \varepsilon_{cr}$ and $\omega \gamma \varepsilon_{cr} E$ and the limit strain at $\lambda_{cu} \varepsilon_{cr}$. Figure 2(b) is the elastic-perfectly plastic reinforcement bar model as defined by normalized parameters: κ and n using stiffness, yield strain, and stress of nE , $\kappa \varepsilon_{cr}$ and $\kappa n \varepsilon_{cr} E$ respectively. As shown in Figure 2(c) area of reinforcement bar is $A_s = \rho b h = \rho b d / \alpha$ by defining $d = \alpha h$. The reinforcement ratio ρ is based on sectional area bh , and differs slightly from the conventional definition of bd in reinforced concrete nomenclature. The depth of compression steel $d = (1 - \alpha)h$, and parameter ζ are introduced such that the area is $A'_s = \zeta A_s = \zeta \rho b h$. Using these definitions, the material models for tension and compression of FRC and steel rebar are converted from standard definitions into dimensionless terms:

$$\sigma_t(\varepsilon_t) = \begin{cases} E\varepsilon_t & 0 \leq \varepsilon_t \leq \varepsilon_{cr} \\ E\varepsilon_{cr} + \eta_1 E(\varepsilon_t - \varepsilon_{cr}) & \varepsilon_{cr} < \varepsilon_t \leq \varepsilon_{trn} \\ \mu E\varepsilon_{cr} & \varepsilon_{trn} < \varepsilon_t \leq \varepsilon_{tu} \\ 0 & \varepsilon_{tu} \leq \varepsilon_t \end{cases}; \quad \frac{\sigma_t(\beta)}{E\varepsilon_{cr}} = \begin{cases} \beta & 0 \leq \beta \leq 1 \\ 1 + \eta_1(\beta - 1) & 1 < \beta \leq \beta_1 \\ \mu & \beta_1 < \beta \leq \beta_{tu} \\ 0 & \beta_{tu} \leq \beta \end{cases} \quad (1)$$

$$\sigma_c(\varepsilon_c) = \begin{cases} \gamma E\varepsilon_c & 0 \leq \varepsilon_c \leq \varepsilon_{cy} \\ \gamma E_c \varepsilon_{cy} & \varepsilon_{cy} < \varepsilon_c \leq \varepsilon_{cu} \\ 0 & \varepsilon_c > \varepsilon_{cu} \end{cases}; \quad \frac{\sigma_c(\lambda)}{E\varepsilon_{cr}} = \begin{cases} \gamma\lambda & 0 \leq \lambda \leq \omega \\ \gamma\omega & \omega < \lambda \leq \lambda_{cu} \\ 0 & \lambda > \lambda_{cu} \end{cases} \quad (2)$$

$$f_s(\varepsilon_s) = \begin{cases} E_s \varepsilon_s & 0 \leq \varepsilon_s \leq \varepsilon_{sy} \\ E_s \varepsilon_{sy} & \varepsilon_s > \varepsilon_{sy} \end{cases}; \quad \frac{f_s(\chi)}{E\varepsilon_{cr}} = \begin{cases} n\chi & 0 \leq \chi \leq \kappa \\ n\kappa & \chi > \kappa \end{cases} \quad (3)$$

Equilibrium of internal forces and moment-curvature using a 1-D internal force equilibrium model are represented by a linear distribution of strain based on the curvature-depth relationship. The average strain in the rebar is defined using the nominal strain distribution by the Kirchhoff assumption. By implementing the linear strain distribution, the stresses, and integrals of stresses to obtain the internal forces. The internal force equilibrium is solved for the neutral axis and the internal moment by the internal force and moment arm from the neutral axis. The normalized maximum tensile strain, β increases uniformly as an independent variable to move from one stage of loading to the other. The derivation of moment-curvature is reported in previous work (Mobasher, Yao, & Soranakom, 2015a; Pleesudjai, 2021). The solutions for the moment M_β and curvature ϕ_β for each range of β , are represented by the normalized cracking values M_{cr} and ϕ_{cr} as:

$$M_\beta = m'_\beta M_{cr}; \quad M_{cr} = \frac{1}{6} b h^2 E \varepsilon_{cr} \quad (4)$$

$$\phi_\beta = \phi'_\beta \phi_{cr}; \quad \phi_{cr} = \frac{2\varepsilon_{cr}}{h} \quad (5)$$

A “Tri-linear” tension, “Bi-linear” compression and rebar stress-strain model is used to construct the moment-curvature envelope of various $M-\phi$ closed form solutions for the different stages by switching from one stage to the other. The envelope curve is the minimum moment among all available options. This transition can be determined by the gradient of the curves at the intersection points, which define the lower moment capacity as seen in Figure 3(a). The rebar in this sample is steel, for the case of GFRP or FRP, the parameters can be modified. The properties of UHPC in Figure 3(b) are conducted in the range of strain-hardening data reported by (Haber et al., 2018).

4. Closed-form Solution for Moment-Curvature in Serviceability

The complete $M-\phi$ response envelope as a function of the strain variable, β , is shown in Figure 3(a) as it begins with the elastic stage in concrete matrix and rebar (Stage 1) until $\beta=1$ where matrix experiences the first cracking, with elastic compression and rebar entering the next stage (Stage 2.1). Further strain increase of the bottom fiber, $1 < \beta \leq \beta_1$ transitions from Stage 2.1 to 2.2 where rebar starts yielding. At this intersection point, the stiffness decreases significantly due to the limited stress provided by rebar, as cracks are formed, and tension stiffening is observed at the major cracks. The response moves to the intersection point between Stage 2.2 to 4.2, the extreme fiber tension reaches the third linear segment of tension model, where $\beta_1 < \beta \leq \beta_{tu}$ while compression zone remains elastic until $\beta = 62$ where compression strain exceeds the elastic strain limit, $\varepsilon_{cy}=0.0025$. The ultimate strain of UHPC compression can be demonstrated and calculated $M-\phi$

response at the ultimate limit state (ULS). More detail on the generalized derivation of and closed-form solution for a complete path of each stage (Stage 1 to 5.2) and model verification can be found in (Pleesudjai, 2021) (Yao, Mobasher, Wang, & Xu, 2020).

A parametric study for various potential material properties of UHPC is conducted to show the effect of compressive strength, rebar content in terms of reinforcement ratio, ρ , as well as the residual tensile strength is shown Figure 4(a), (b), and (c) respectively. Note that the compressive strength for the under-reinforced sections has almost no effect in the response, whereas the moment capacity can be increased significantly by increasing either the reinforcement ratio or the residual tensile strength due to the use of fibers. The allowable compressive strain is limited at $\epsilon_c=0.004$. As the moment capacity increase, ductility is slightly reduced.

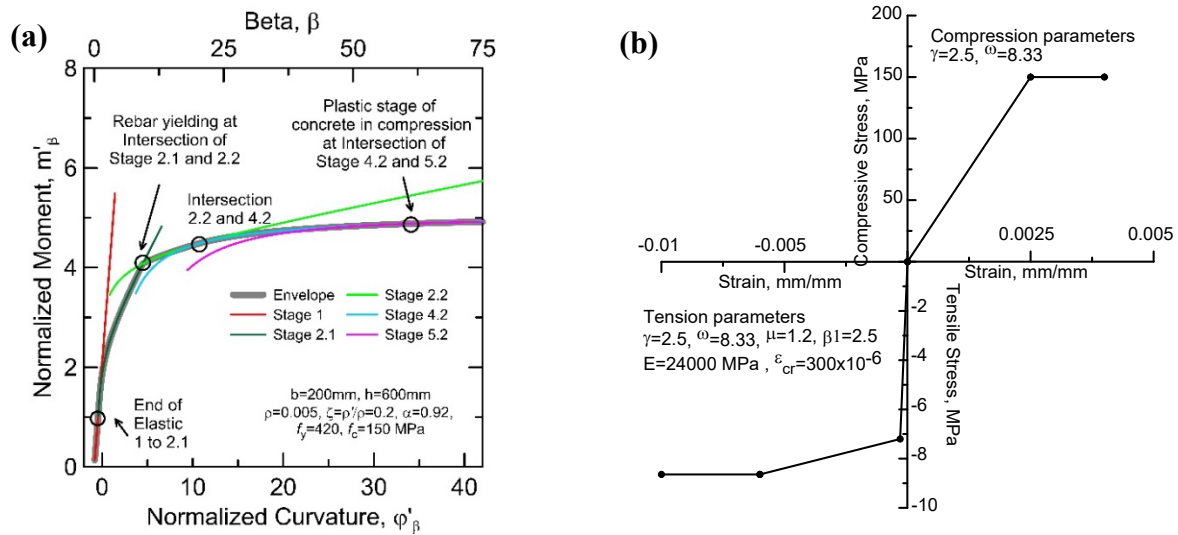


Figure 3. (a) Moment-Curvature responses and envelope curve (b) σ - ϵ response of UHPC with the input parameters.

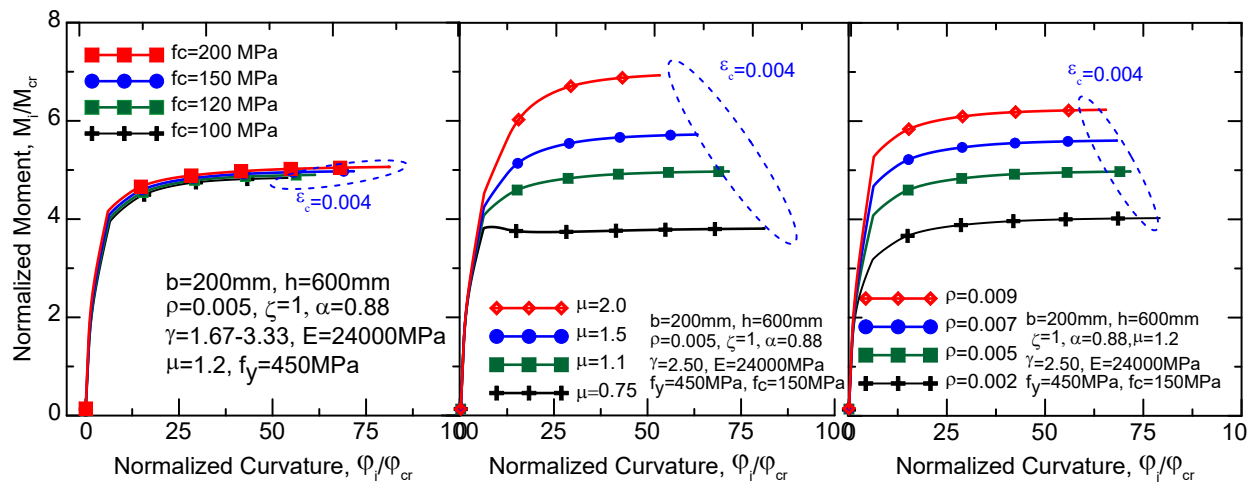


Figure 4. Parametric study of the effect of compressive strength, residual tensile strength, and reinforcement ratio on the normalized moment-curvature response of UHPC beams

5. Generalized Approach for Computing Load-Deflection Response

A generalized approach for the calculation of the load-deflection response for full-field rotation and deflection of general beams has been developed to take advantage of the parametric moment-Curvature simulation (Yao, Aswani, Wang, & Mobasher, 2018). In addition to the computation of the load-deflection response, these solutions provide detailed derivations for various stages of first cracking, δ_c , at first bilinear cracking δ_{bcr} , and at ultimate δ_u . The size of the characteristic length L_p needs to be specified in order to simulate the localization in the post-peak range. The primary input into this algorithm is the linearized representation of the parametric variables obtained from the normalized moment-curvature envelop to compute the rotation and deflection parameters based on dimensions, loading geometry, and basic material properties.

6. Hybrid UHPC

The design of reinforced concrete members for durability aspects such as bridge decks, or environmental structures is typically governed by the serviceability state rather than the ultimate state. This necessitates verifying the stress distribution at any given strain, or crack width, as well as the deflection profile, crack depth, and location of the neutral axis at service load. There is an interaction between two types of reinforcement by the fibers and rebars as the activation of each phase is by means of the fracture of matrix. These interactions occur at different stages of deformation and studying them can be beneficial (Yao et al., 2018). The coefficients for values of $n=7.7$ and $\gamma=2.1$, $\omega=11.67$ are used to simplify the equations. The moment-curvature response can be divided into three main stages, elastic, transitional elastic-plastic, and perfectly plastic by generating the moment-curvature interactions and curves using the closed-form solutions provided in (Mobasher et al., 2015a)(Pleesudjai, 2021). These plots are obtained in a straightforward manner and the effect of various combinations of rebar and fiber content can be simulated into one diagram as shown. The relative contribution of each component is also shown in Figure 5.

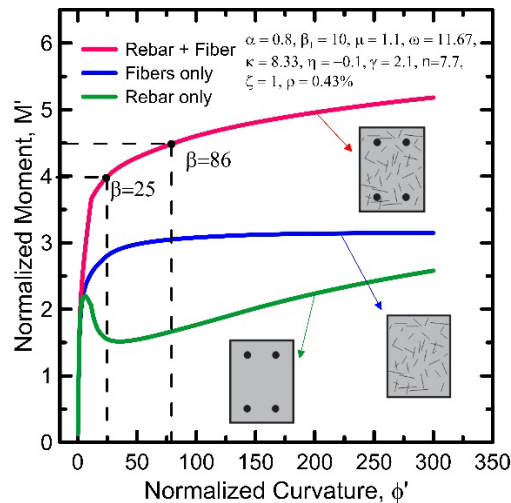


Figure 5. Simulated Moment-Curvature Response for UHPC comparing HRC with plain FRC and conventional rebar design

Figure 5 shows the parametric modeling of the relative contribution of the matrix with fibers and rebars to the full load-carrying capacity of a reinforced section. The simulation is conducted under the conditions of perfect bond of rebar. If the matrix is only reinforced with rebar, its contribution

terminates at the cracking point, and all of the load is transferred to the rebar at the crack. However, if the matrix is also capable of carrying loads, the load transition of the rebar is gradual as the tensile capacity of the matrix is also utilized. The simulation shows that if the matrix is capable to carry only 30% of its tensile strength in the post-peak response by means of a hybrid design using short fibers in the UHPC, then the load carried by the reinforcement is reduced by 50%, or the reinforcing effect is doubled in efficiency and the moment capacity is doubled at the yielding of the reinforcement.

Design Example Problem Addressing the Serviceability Approach

Use various serviceability measures to design for the maximum moment capacity of a simply supported doubly-reinforced UHPC beam with a span of $L=7$ ft and a rectangular Section 12" deep x 6" wide. Use strength of $f'_c=23$ ksi, with $\rho = 0.43\%$, Steel properties are $E_s = 30 \times 10^6$ psi, $f_y = 60$ ksi and $\varepsilon_s = 0.002$. The rebar has 2.5" cover at top and bottom. Using parameters from normalized response shown in Figure 5, we obtain geometric and material parameters:

$$L = 7 \text{ ft}, b = 6", h = 12", f'_c = 23 \text{ ksi} \text{ Considering } \alpha = (12'' - 2.5'')/12'' = 0.8$$

$$\text{Assume } \gamma = 1, E = E_c = 57000\sqrt{f'_c} = 8644 \text{ ksi}, \text{ and } \sigma_{cr} = f'_t = 6.7\sqrt{f'_c} = 6.7\sqrt{23000} = 1016 \text{ psi}$$

$$\varepsilon_{cr} = \frac{\sigma_{cr}}{E} = \frac{1016 \text{ psi}}{8644 \text{ ksi}} = 117 * 10^{-6}, \varepsilon_s = \frac{F_y}{E} = \frac{60}{29,000} = 0.002$$

$$\omega = \frac{f'_c}{f'_t} = \frac{f'_c}{\varepsilon_{cr} E} = \frac{23}{(117 \times 10^{-6}) \times 8644} = 22.7, \kappa = \frac{f_{sy}}{n E \varepsilon_{cr}} = \frac{60000}{7.7 \times 8644000 \times 0.000117} = 7.7$$

$$M_{cr} = \frac{1}{6} \sigma_{cr} b h^2 = \frac{1}{6 \times 12} (1016 \text{ psi}) \times 6'' \times (12'')^2 = 12.9 \text{ k-ft (17.47 kN-m)}, \varphi_{cr} = \frac{M_{cr}}{EI} = 2 \times 10^{-5}$$

Case 1-Calculation of the maximum moment capacity

Generating normalized $M-\varphi$ curve based on given parameters as shown in Figure 5. The max moment for this geometry from Figure 5 is $M' = 5.2$. The maximum moment capacity is:

$$M = M' \times M_{cr} = 5.2 \times 12.9 \text{ kips-ft} = 67.1 \text{ kips-ft (91 kN-m)}$$

Case 2-Allowable Moment for maximum strain in tension no greater than $\varepsilon = 1\%$

Use Figure 5 with the tension strain, $\beta = 0.01/\varepsilon_{cr} = 86$, the normalized moment, M' is 4.5.

$$M = M' \times M_{cr} = 4.5 \times 12.9 \text{ kips-ft} = 58.05 \text{ kips-ft (78.7 kN-m)}$$

Case 3-Design for maximum allowable curvature in tension of $\varphi = 0.5 \times 10^{-4} \text{ in}^{-1}$

$$\varphi' = \frac{\varphi}{\varphi_{cr}} = \frac{0.0005}{0.00002} = 25, \text{ get } M' = 4.1, M = M' M_{cr} = 52.9 \text{ kips-ft (71.7 kN-m)}$$

7. Conclusion

An approach developed closed form solutions establishes the envelop moment-curvature response and can be used to validate the various limit states in terms of flexural load, stresses, curvature, and strain as well as deflection, shear, and fatigue. Results show that one can reduce the amount of reinforcement for UHPC and allow fibers in the matrix to compensate for the post-crack stiffness as well as the load-carrying capacity of hybrid UHPC. This proposed solution can be used to minimize section geometry and minimized the use of concrete and material properties to achieve the desired capacity, especially in the serviceability stage.

References

- El-Helou, R. G., & Graybeal, B. A. (2021). *The Ultra Girder: A Design Concept for a 300-foot Single Span Prestressed Ultra-High Performance Concrete Bridge Girder*. 1–9. <https://doi.org/10.21838/uhpc.9707>
- Haber, Z. B., Varga, I. D. la, Graybeal, B. A., Nakashoji, B., & El-Helou, R. (2018). Properties and Behavior of UHPC-Class Materials. *Fhwa-Hrt-18-036*, (March), 153.
- Le Hoang, A., & Fehling, E. (2017). Influence of steel fiber content and aspect ratio on the uniaxial tensile and compressive behavior of ultra high performance concrete. *Construction and Building Materials*, *153*, 790–806. <https://doi.org/10.1016/j.conbuildmat.2017.07.130>
- Mobasher, B., Li, A., Yao, Y., Arora, A., & Neithalath, N. (2021). Characterization of toughening mechanisms in UHPC through image correlation and inverse analysis of flexural results. *Cement and Concrete Composites*, *122*, 104157. <https://doi.org/10.1016/j.cemconcomp.2021.104157>
- Mobasher, B., Yao, Y., & Soranakom, C. (2015a). Analytical solutions for flexural design of hybrid steel fiber reinforced concrete beams. *Engineering Structures*, *100*, 164–177. <https://doi.org/10.1016/j.engstruct.2015.06.006>
- Mobasher, B., Yao, Y., & Soranakom, C. (2015b). Analytical solutions for flexural design of hybrid steel fiber reinforced concrete beams. *Engineering Structures*, *100*, 164–177. <https://doi.org/10.1016/j.engstruct.2015.06.006>
- Pleesudjai, C. (2021). *Generalized modeling and Experimental Validation of Flexural Response in Cement Based Composites*. Arizona State University.
- Wille, K., & Naaman, A. E. (2012). Pullout behavior of high-strength steel fibers embedded in ultra-high-performance concrete. *ACI Materials Journal*, *109*(4), 479–488. <https://doi.org/10.14359/51683923>
- Yao, Y., Aswani, K., Wang, X., & Mobasher, B. (2018). Analytical displacement solutions for statically determinate beams based on a trilinear moment–curvature model. *Structural Concrete*. <https://doi.org/10.1002/suco.201700150>
- Yao, Y., Mobasher, B., Wang, J., & Xu, Q. (2020). Analytical approach for the design of flexural elements made of reinforced <scp>ultra-high</scp> performance concrete. *Structural Concrete*, *suco.201900404*. <https://doi.org/10.1002/suco.201900404>